Proceedings of the XVI ECSMGE
Geotechnical Engineering for Infrastructure and Development
ISBN 978-0-7277-6067-8

doi:10.1680/ecsmge.60678

Numerical interpretation of the coupled hydro-mechanical behaviour of expansive clays in constant volume column tests

Interprétation numérique du comportement hydromécanique d'argiles expansibles lors de test en colonnes à volume constant

V. Mantikos[*1], A. Tsiampousi[2] , D.M.G. Taborda[2] and D.M. Potts[2]

[1] *Swanton Consulting Ltd, London, United Kingdom*
[2] *Department of Civil and Environmental Engineering, Imperial College, London, United Kingdom*
[*] *Corresponding Author*

ABSTRACT Experimental and numerical studies of the behaviour of expansive clays have been attracting increasing interest, due to their good sealing properties, which render them ideal to be used as engineered barriers (buffers) in both active (e.g. nuclear) and non-active waste disposal facilities. Both large scale and laboratory scaled experiments indicate that the sealing capabilities of the buffer are fundamentally governed by its volumetric behaviour when wetted. In this paper, a constant volume column infiltration test, performed under isothermal conditions on compacted MX80 bentonite, is modelled numerically using the Imperial College Finite Element Program (ICFEP). A modified version of the Barcelona Basic Model is used to simulate the behaviour of the buffer, which is inherently partly saturated. The numerical results agree well with the observed experimental data, especially with regard to the advancement of the wetting front. A detailed interpretation of the computed evolutions with time of stress state, suction and void ratio at different elevations along the sample's axis is carried out, providing insight into the complex hydro-mechanical response of the buffer during the experiment. Indeed, even though the overall volume of the sample was kept constant, a region of localised dilation, which induced the contraction of other zones of the material, was observed to advance simultaneously with the wetting front along the height of the soil column.

RÉSUMÉ Des études expérimentales et numériques du comportement d'argiles expansibles attirent un intérêt croissant dû à leurs bonnes propriétés d'étanchéité qui les rendent idéales en tant que barrières (tampons) conçues au sein d'installations d'entrepôt de déchets actifs (nucléaires par exemple) ou passifs. Des expériences grandeur nature ou à échelle réduite en laboratoire indiquent que les capacités d'étanchéité du tampon sont fondamentalement gouvernées par son comportement volumétrique lors du mouillage. Dans cette étude, un test d'infiltration en colonne à volume constant, accompli sous conditions isothermes sur de la bentonite MX80 compactée est modélisé numériquement à l'aide du programme élément fini ICFEP (Imperial College Finite Element Program). Une version modifiée du modèle classique de Barcelone (Barcelona Basic Model) est utilisé pour simuler le comportement du tampon, qui est intrinsèquement en partie saturé. Les résultats numériques sont en bon accord avec les données expérimentales, en particulier en ce qui concerne la progression du front mouillé. Une interprétation détaillée des évolutions calculées en fonction du temps de l'état de stress, de l'aspiration et du rapport du vide à plusieurs endroits le long de l'axe de l'échantillon ont été réalisées, fournissant d'importantes informations concernant la réponse hydromécanique complexe du tampon pendant l'expérience. En effet, bien que le volume global de l'échantillon fût maintenu constant, une région de dilatation localisée induisant une contraction d'autres zones de l'échantillon a été observée avançant en même temps que le front mouillé le long de la hauteur de la colonne de bentonite.

1 INTRODUCTION

Deep geological disposal is a permanent method of disposing of high level nuclear waste and it gains support from researchers for being the safest option. The function of a buffer in the sealing arrangement is to isolate the waste canister from erosion, mechanical loading and radionuclide transfer. In-depth investigation of the fundamental behaviour of expansive clays is in progress in all nuclear power generating countries to model and assess their performance as a buffer material.

Of particular research interest is the re-saturation of the buffer under constrained swelling conditions. Different theoretical approaches have addressed the mechanical aspect of this phenomenon through a suction dependent stress state surface (Gens & Alonso, 1992), often incorporating a double structure (Alonso et al. 1999) or a generalised plasticity model (Sanchez et al. 2005). Moreover, vapour diffusion (Kröhn 2005) or liquid water flow (Hoffmann et al. 2007) theories may be used to explain the hydration process. The thermal and chemical effects that add to the complexity of the problem are not discussed here.

To increase confidence in modelling the coupled behaviour, full scale field and laboratory tests were carried out (Schanz et al. 2013). Laboratory tests include constant suction or constant stress conditions, free swell tests or constant volume hydration tests. Schanz et al. (2008) propose a sensitivity analysis procedure to identify the important modelling parameters using swell test data.

The unsaturated hydraulic permeability of clays is most suitably measured by unsteady methods (Benson et al. 1997; Cui et al. 2008). One common test for bentonite buffers is the column infiltration technique (swell test), where a cylindrical specimen is wetted at one end. This test simulates the confined hydration conditions in the buffer, enabling the study of the evolution in density and permeability as hydration progresses along the column (Delage et al. 2010).

In this paper, a constant volume column infiltration test (Marcial et al. 2008), performed under isothermal conditions on compacted MX80 bentonite, is modelled numerically using the Imperial College Finite Element Program (ICFEP) (Potts & Zdravkovic 1999). A modified version of the Barcelona Basic Model (BBM) (Georgiadis et al. 2005, Tsiampousi et al. 2013) is used to simulate the behaviour of the buffer, which is inherently partly saturated.

2 SIMULATED INFILTRATION TEST

The hydration test described by Marcial et al. (2008) was selected for the purpose of acting as a reference model for the numerical analysis results. The test was conducted under iso-thermal conditions, at T=20^o C. The soil material was subjected to a 39MPa static compaction stress to achieve a density of 1.7 Mg/m^3 after rebound, so that it would have a high swelling potential and a double porosity structure. The water content was measured at 8.2%, which corresponds to 103MPa suction. The specimen was prepared with a diameter slightly smaller than the apparatus cylinder to avoid friction developing during placement. Figure 1 presents the arrangement of the apparatus.

The sample was placed inside a 50mm diameter x 250mm long rigid cylinder in the form of compacted bricks and the system was sealed and thermally isolated. The radial stress was interpreted by Marcial et al. (2008) from the deformation of thin semi-rigid zones of the cylinder, calibrated so that 60MPa of pressure gave 5μm deflection. Relative Humidity (RH) probes where placed at distances of 4.5cm, 9.5cm, 14.5cm, 19.5cm and 25cm from the base of the sample.

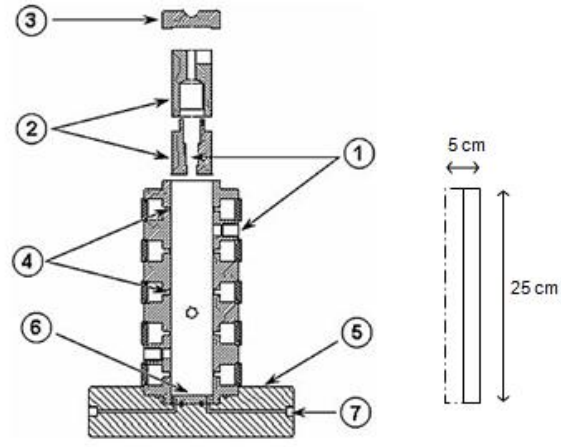

Figure 1. Infiltration column: (1) holes for RH sensors location (2) split head piston (3) piston cap (4) 2mm thick zones for lateral stress monitoring (5) column base (6) porous stone (7) water intake circuit. (Marcial et al. 2008).

3 NUMERICAL MODEL

3.1 Finite element mesh

Quadrilateral 8-noded isoparametric elements were used for the discretisation of the sample. Displacement degrees of freedom were assigned to all nodes, whereas pore water pressure (PWP) degrees of freedom were assigned only to corner nodes.

3.2 *Boundary conditions*

In order to force constant volume conditions, no radial displacements were allowed along the left and right vertical boundaries of the finite element mesh and no vertical displacements along the horizontal top and bottom boundaries.

All boundaries have been considered impermeable, with the exception of the bottom boundary where a constant water pressure of 10kPa was prescribed to simulate water infiltration.

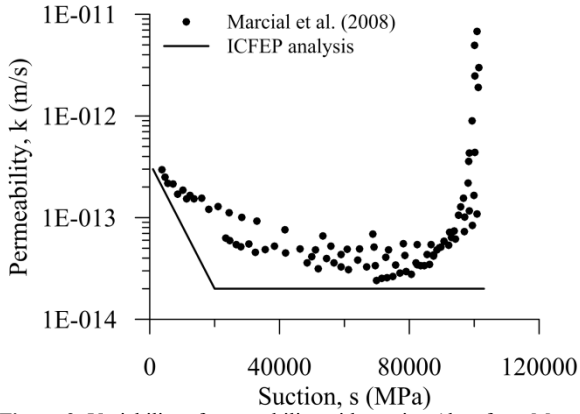

Figure 2. Variability of permeability with suction (data from Marcial et al., 2008).

3.3 *Constitutive, water retention and permeability models*

The material used for the experiment was MX 80, a commercial bentonite from Wyoming, USA. It is a Na-smectite with some Ca (Delage et al. 2010), high montmorillonite content (80%), high liquid limit and specific surface, making it a highly expansive clay.

The Barcelona Basic model (Alonso et al. 1990) was used as the constitutive model for the analysis, with the modifications proposed by Georgiadis et al. (2005) and Tsiampousi et al. (2013), in conjunction with a Van Genuchten (1980)-type soil-water retention curve (SWRC). The respective model parameters are summarised in Table 1 and were calibrated based on laboratory data reported by Tang et al. (2008) and Dueck (2008).

The variation of permeability, k, with suction, s, adopted in the analysis is shown in Figure 2, in comparison with experimental data from Marcial et al. (2008). In the analysis, the logarithm of permeability varies linearly with suction, from its saturated value k_{sat} corresponding to suction p_1 to a minimum value k_{min} at suction p_2 (values in Table 1).

Table 1. Values of parameters used in model

Parameter	Value	Unit	Description
Seepage properties			
k_{sat}	3e-13	m/s	Saturated permeability
k_{min}	0.2e-13	m/s	Minimum permeability
p_1	1000	kPa	Pore pressures at which permeability starts changing
p_2	20000	kPa	Pore pressures at which permeability ceases changing
Mechanical parameters			
$\alpha_g = \alpha_f$	0.4		Model parameter controlling YS an PP shape
$\mu_g = \mu_f$	0.9		Model parameter controlling YS an PP shape
$M_g = M_f$	0.35		Generalised normalised stress ratio in critical state
p_c	24.6	kPa	Characteristic pressure
v_1	2.54		Specific volume at mean net stress p = 1kPa
$\lambda(0)$	0.25		Fully saturated compressibility coefficient
κ	0.01		Elastic compressibility coefficient
r	0.33		Maximum soil stiffness parameter
B	3.8E-5	1/kPa	Soil stiffness increase parameter
κ_s	0.231		Elastic compressibility coefficient for changes in suction
χ	1.0		Parameters controlling the variation of elastic compressibility coefficient with degree of saturation
ω	0.0		
μ	0.4		Poison ratio
s_0	400000	kPa	Yield value of suction
λ_s	0.3		Plastic compressibility coefficient for changes in suction
SWRC			
s_{air}	1000	kPa	Air entry suction
α	2.8E-5		Fitting parameter
n	1.3		Fitting parameter
m	1		Fitting parameter
S_{r0}	0.15		Residual degree of saturation

3.4 Initial conditions/stress state

The compaction-induced suction was 103 MPa, corresponding to an initial degree of saturation of 32.3%. No load was initially applied ($\sigma_r = \sigma_v = 0$) resulting in a compressive initial mean effective stress which is equal to the induced suction. The initial void ratio was set to 0.66.

3.5 Type of analysis

The infiltration test described above was simulated in a hydro-mechanical (HM) coupled consolidation, partly saturated, axi-symmetric analysis. The Imperial Finite Element Program (ICFEP) (Potts & Zdravkovic 1999) was used, which employs a modified Newton-Raphson solution technique with an error controlled sub-stepping stress-point algorithm.

ICFEP uses a sign convention for the stresses where tension is considered positive. This applies also for the pore water pressures, i.e. suction has a positive sign. The same convention is used herein. As consolidation is a time-dependent process, time steps were assigned to each increment. Each of the first 60 increments corresponds to one minute of simulated time, each of the next 23 increments correspond to one hour and after increment 84 the time step was set to one day. The duration of the test was 208 days, modelled in 290 increments.

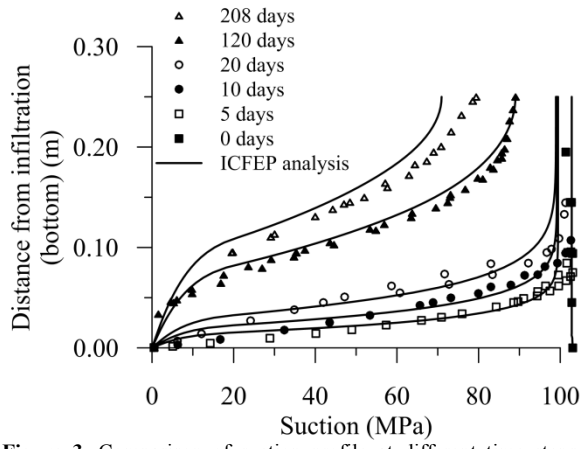

Figure 3. Comparison of suction profile at different time steps with laboratory data from Marcial et. al (2008).

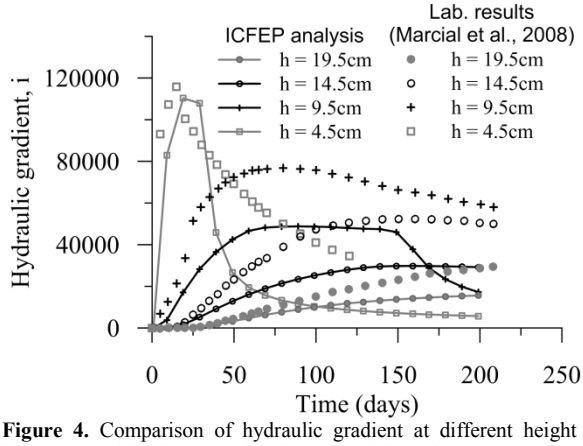

Figure 4. Comparison of hydraulic gradient at different height increments with laboratory data from Marcial et. al (2008).

4 COMPARISON WITH EXPERIMENTAL DATA

The numerical results are compared to the experimental data given by Marcial et al. (2008) in figures 3 and 4. Figure 3 presents the evolution of suction with time along the height of the sample. The numerical predictions are in good agreement with the measured data. Furthermore, the hydraulic gradient at different heights derived from the numerical analysis evolves with time in a manner qualitatively similar to that observed in the laboratory test (Figure 4).

5 INTERPRETATION OF PREDICTED BEHAVIOUR

Figures 5 and 6 illustrate the stress path at a Gauss point located at a distance of 14.75mm from the bottom boundary of the mesh (infiltration boundary), on the mean net stress-suction (p-s) and mean net stress-deviatoric stress (p-q) planes, respectively. Figure 7 illustrates the evolution of void ratio with time at various distances from the infiltration boundary. Examination of the three figures provides a better insight into the mechanisms controlling the behaviour of the column of soil and contributes to a more comprehensive explanation of the observed results.

The initial stress state of the particular Gauss point studied is represented by point (a). As water infiltrates the base of the sample, the saturation front gradually advances upwards. The soil below the satu-

ration front swells, causing local compression above the saturation front. Therefore, the soil at a given cross-section initially compresses slightly and starts swelling only when the saturation front has reached this section. The initial small decrease in void ratio is associated with the sample being initially sheared in compression, as indicated by the path from (a) to (b) in Figure 6. This is followed by shearing in extension ((b) to (c)) when the wetting front has advanced enough for the current cross-section to swell. Concurrently, suction reduces due to infiltration of water and therefore the yield surface (Y.S.) in the p-q plane shrinks. This is indicated by the reduction in the preconsolidation mean stress, p_0, at the current value of suction, as shown in Figures 5 and 6. As shearing in extension continues, the stress path yields on the Y.S. at point (c). At this particular instance, yielding has occurred only on the p-q plane (Figure 6) and not on the s-p plane (Figure 5). Although the stress path yields on the wet side of critical state, the Y.S. keeps on shrinking due to further reduction in suction, which dominates the behaviour, and the stress path reverses in direction but always remains on the Y.S. in the p-q plane. At point (d) where q=0, the soil collapses, the void ratio reduces dramatically (Figure 7) and the stress path is simultaneously on the loading-collapse (L.C.) curve on the s-p plane (Figure 6) and the Y.S. on the p-q plane (Figure 5).

From (c) to (d) the L.C. has moved as a result of plasticity having been induced in the p-q plane. As discussed above, p_0 has decreased. Nonetheless, because of yielding on the wet side, p_0*, which is the preconsolidation mean stress defined at zero suction, has increased, meaning that the new L.C. at the instance of first wetting-induced collapse plots to the right of the initial one in Figure 5. Note that the hardening parameter of the model is p_0* and not p_0.

In Figure 7 it can be seen that the void ratio keeps increasing until the cross-section collapses upon reaching the L.C. curve. As saturation continues, the front of wetting-induced collapse advances upwards with the saturation front, allowing sections beneath it (i.e. h=3cm) to swell again. This results in a wave-like evolution of void ratio within the sample.

Figure 8 illustrates the stress paths on the s-p plane at different heights along the soil column. They all exhibit a similar shape, which further supports the above discussion. In Figure 8, the initial stress point (a), the point where the direction of shearing changes from compression to extension (b), the yielding point on the q-p plane (c) and the point of collapse (d) are all shown.

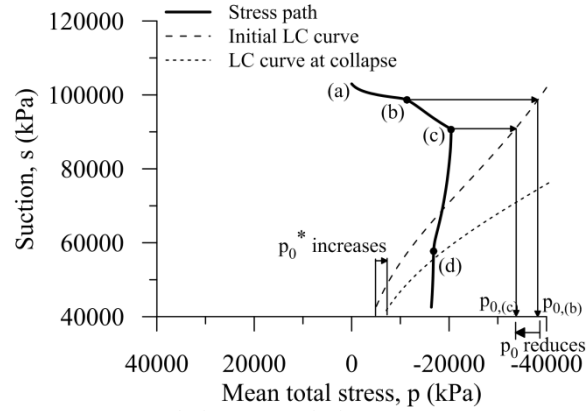

Figure 5. Stress paths in s-p space for h = 14.75mm.

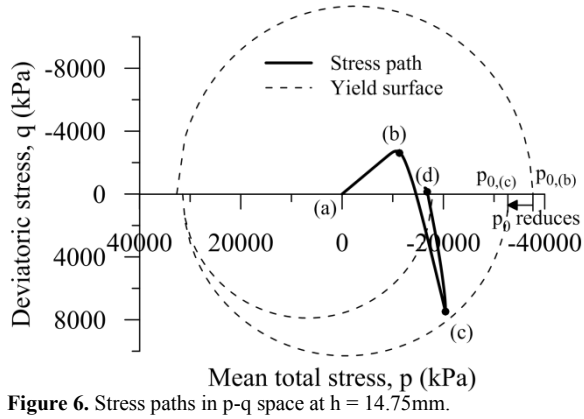

Figure 6. Stress paths in p-q space at h = 14.75mm.

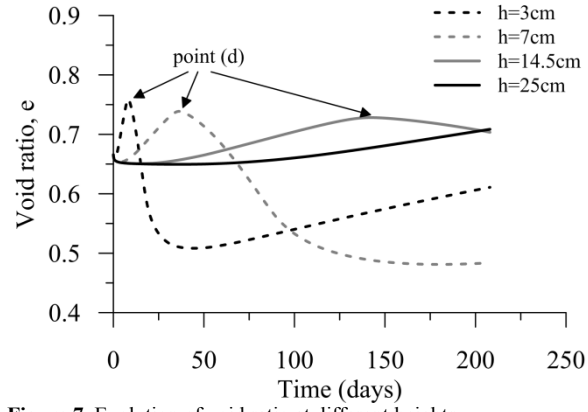

Figure 7. Evolution of void ratio at different heights.

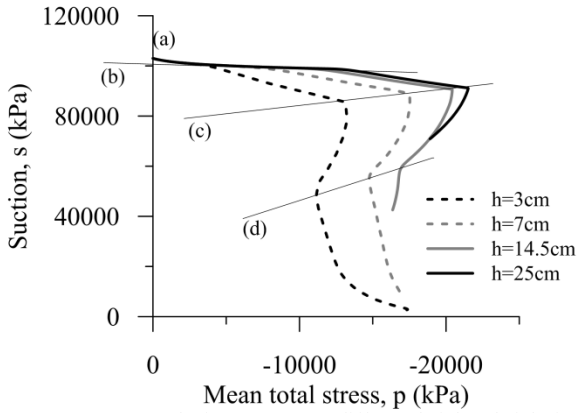

Figure 8. Stress paths in s-p space at different heights (height increasing from left to right).

6 CONCLUSIONS

Many processes happen simultaneously within the buffer, even if thermal phenomena are ignored. An attempt is made to identify and interpret them. Despite neglecting the effect of a double porosity structure, the analysis successfully provided insight into the complex response of bentonite when hydrated, helping identify mechanisms within the buffer which would otherwise be concealed.

The results show that the propagation of the water front is a time-dependent process, leading to alternate compression/swelling. As a result, it has been demonstrated that soil along the axis of the buffer exists at different void ratios and stress states. Moreover, as compacted bentonite is highly expansive, swelling-induced stresses were shown to be high enough to cause yielding in terms of deviatoric stress, while collapse occurs under reducing suction.

REFERENCES

Alonso, E. E., Gens, A. & Josa, A. 1990, A constitutive model for partially saturated soils, *Géotechnique* **40** (3), 405-430.

Alonso, E. E., Vaunat, J. & Gens, A. 1999. Modelling the mechanical behaviour of expansive clays, *Engineering Geology* **54** (1-2), 173-183.

Benson, C. H. & Gribb, M. M. 1997. Measuring unsaturated hydraulic conductivity in the laboratory and field, *Proceedings of the 1997 1st Geo-Institute Conference,* 113-168. ASCE, Logan, UT, USA.

Cui, Y. J., Tang, A. M., Loiseau, C. & Delage, P. 2008. Determining the unsaturated hydraulic conductivity of a compacted sand-bentonite mixture under constant-volume and free-swell conditions, *Physics and Chemistry of the Earth* **33**, S462-S471.

Delage, P., Cui, Y. & Tang, A. 2010. Clays in radioactive waste disposal, *Journal of Rock Mechanics and Geotechnical Engineering* **2** (2), 111-123.

Dueck, A. 2008. Laboratory results from hydro-mechanical tests on a water unsaturated bentonite, *Engineering Geology* **97** (1–2), 15-24.

Gens, A. & Alonso, E. E. 1992. A framework for the behaviour of unsaturated expansive clays, *Canadian Geotechnical Journal* **29** (6), 1013-1032.

Georgiadis, K., Potts, D. M. & Zdravkovic, L. 2005. Three-dimensional constitutive model for partially and fully saturated soils, *International Journal of Geomechanics* **5** (3), 244-255

Hoffmann, C., Alonso, E. E. & Romero, E. 2007. Hydro-mechanical behaviour of bentonite pellet mixtures, *Physics and Chemistry of the Earth, Parts A/B/C* **32** (8–14), 832-849.

Kröhn, K. 2005. New evidence for the dominance of vapour diffusion during the re-saturation of compacted bentonite, *Engineering Geology* **82** (2), 127-132.

Lagioia, R., Puzrin, A. M. & Potts, D. M. 1996. A new versatile expression for yield and plastic potential surfaces, *Computers and Geotechnics* **19** (3), 171-191.

Marcial, D., Delage, P. & Cui, Y. J. 2008. Hydromechanical couplings in confined MX80 bentonite during hydration. *1st European Conference on Unsaturated Soils, E-UNSAT 2008*, 249-255. CRC Press, Durham, United kingdom.

Potts, D. M. & Zdravkovic, L. 1999. *Finite element analysis in geotechnical engineering. theory.* London, Thomas Telford.

Sanchez, M., Gens, A., do, N. G. & Olivella, S. 2005. A double structure generalized plasticity model for expansive materials, *International Journal for Numerical and Analytical Methods in Geomechanics* **29** (8), 751-787.

Schanz, T., Datcheva, M. & Zimmerer, M. 2008. Identification of coupled hydro-mechanical parameters with application to engineered barrier systems, *1st European Conference on Unsaturated Soils, E-UNSAT 2008,* 797-803. CRC Press, Durham, United kingdom.

Schanz, T., Long Nguyen-Tuan & Datcheva, M. 2013. A Column Experiment to Study the Thermo-Hydro-Mechanical Behaviour of Expansive Soils, *Rock Mechanics and Rock Engineering* **46** (6), 1287-301.

Tang, A. M., Cui, Y. J. & Barnel, N. 2008. Compression-induced suction change in a compacted expansive clay. *1st European Conference on Unsaturated Soils, E-UNSAT 2008,* 369-374. CRC Press, Durham, United kingdom.

Tsiampousi, A., Zdravkovic, L. & Potts, D. M. 2013. A three-dimensional hysteretic soil-water retention curve, *Geotechnique.* **63** (2), 155-164.

Van Genuchten, M. T. 1980. A closed-form equation for predicting the hydarulic conductivity of unsaturated soils. *Soil Sci. Soc. Am. J.* **44**, 892-898.